ORIGINAL ARTICLE—ALIMENTARY TRACT

Differential effects of nutritional and non-nutritional therapies on intestinal barrier function in an in vitro model

Lily Nahidi · Andrew S. Day · Daniel A. Lemberg · Steven T. Leach

Abstract

Background Diminished intestinal epithelial barrier function contributes to the pathogenesis of Crohn's disease. Clinical and experimental studies propose that increased tumor necrosis factor (TNF)-α promotes barrier dysfunction. The aim of this study was to investigate the effects of nutritional and other therapies upon intestinal barrier function in the presence of TNF-α in an in vitro model.

Methods Caco-2 monolayers were grown to confluence on membrane supports and then exposed to TNF-α in the presence of polymeric formula, hydrocortisone or infliximab. Monolayer permeability was evaluated by measuring epithelial resistance, short-circuit current and horseradish peroxidase flux in an Ussing chamber. Tight junction and myosin II regulatory light-chain kinase gene expression was analysed by real-time PCR, with protein expression and localization analysed by Western blot and immunofluorescence.

Results TNF-α increased monolayer permeability and diminished tight junction integrity. However both polymeric formula and infliximab completely abrogated the effects of TNF-α. These monolayers displayed unchanged permeability and tight junction integrity compared to untreated cells (media-no-TNF-α controls). In contrast, hydrocortisone only partially abrogated the effects of TNF-α, with these monolayers having increased permeability and altered tight junction integrity compared to media-no-TNF-α controls.

Conclusions Both polymeric formula and infliximab completely prevent epithelial barrier dysfunction in the presence of TNF-α, whereas hydrocortisone partially prevents barrier dysfunction. These results provide evidence that superior mucosal healing can be achieved with both polymeric formula and infliximab compared to hydrocortisone.

Keywords Crohn's disease · Nutritional therapy · Polymeric formula · Hydrocortisone · Infliximab · Intestinal epithelial permeability

L. Nahidi · A. S. Day · S. T. Leach (✉)
School of Women's and Children's Health,
University of New South Wales, Randwick,
Sydney, NSW, Australia
e-mail: s.leach@unsw.edu.au

L. Nahidi
e-mail: lily.nahidi@student.unsw.edu.au

A. S. Day
Paediatric Gastroenterology, Christchurch Hospital,
Christchurch, New Zealand
e-mail: andrew.day@otago.ac.nz

A. S. Day
Department of Paediatrics, University of Otago, Christchurch,
Christchurch, New Zealand

D. A. Lemberg
Department of Gastroenterology,
Sydney Children's Hospital, Randwick, Sydney, NSW, Australia
e-mail: Daniel.Lemberg@sesiahs.health.nsw.gov.au

Introduction

Crohn's disease (CD) and ulcerative colitis (UC) are inflammatory bowel diseases (IBD) of the gastrointestinal

tract with diarrhoea as a principal symptom [1, 2]. Decreased epithelial barrier function and increased intestinal para-cellular permeability contributes to IBD pathogenesis. However, the intracellular mechanisms involved in intestinal barrier dysfunction are not yet fully explained.

The healthy intestinal barrier consists of a monolayer of epithelial cells connected by tight junctions, crucial for para-cellular transport of ions, nutrients and water across the mucosa and the exclusion of pathogens and other toxic substances [1, 3]. Tight junctions are multiple protein complexes, with two classes of transmembrane proteins (claudin and occludin) forming the molecular basis of tight junctions in epithelial cells [1, 3]. These proteins interact with cytoplasmic proteins [zonula occludens (ZO), F-actin filaments and myosin II] to attach the tight junction strands to the cytoskeleton [1, 3]. The correct association of these proteins is important in maintaining normal epithelial barrier function. In IBD, epithelial barrier function is impaired and manifests as increased intestinal permeability [1, 3]. Pro-inflammatory mediators such as tumor necrosis factor (TNF)-α influence tight junction morphology, structure and gene expression, as is evident in patients with CD [2]. The diminished tight junction function allows para-cellular penetration of noxious luminal antigens, which promote gastrointestinal mucosal injury and inflammation. However, whether barrier malfunctions precede IBD or are consequent to active inflammation is unclear.

Chronic inflammation also impacts the nutritional status of patients with IBD, especially in childhood [4]. Micronutrient and vitamin deficiencies, weight loss and delayed pubertal development are commonly associated with childhood IBD [4]. The reasons for this are multi-factorial and include diminished intake, nutrient loss and malabsorption. Therefore, nutritional supports, as well as reducing inflammation, are targets of current therapies for CD.

The identification of TNF-α as central in the pathogenesis of intestinal inflammation led to the development of anti-TNF-α agents, such as infliximab (IFX), as treatments for CD. IFX effectively reduces inflammation and leads to high rates of mucosal healing [5, 6]. However, it is associated with side effects [7] including increased risk of infection and hepatosplenic T cell lymphoma [8]. Corticosteroids such as prednisone or hydrocortisone (HC) also effectively induce clinical remission in patients with CD [7, 9, 10]. However, corticosteroids are also associated with side effects including those related to growth and nutrition [7, 10], and corticosteroids lead to only low rates of mucosal healing [9, 10]. Polymeric formula (PF), when used as an exclusive nutritional source, is as effective as steroid therapy in inducing remission in children with CD [9–11]. Like IFX, PF leads to high rates of mucosal

healing [9, 10], provides nutritional improvements, reduces pro-inflammatory cytokines [10, 12] and enhances anti-inflammatory cytokines with minimal side effects [4, 10].

In the current study, we examine the hypothesis that TNF-α reduces tight junction integrity and reduces epithelial barrier function. Our aim was to examine how three CD therapies (PF, IFX and HC) protect tight junction integrity and prevent epithelial barrier dysfunction in the presence of TNF-α and therefore promote mucosal healing.

Materials and methods

Reagents

Polymerase chain reaction (PCR) primers (Invitrogen, Carlsbad, CA, USA); rhTNF-α, HC and basic reagents (Sigma Chemical Company, St Louis, MO, USA); IFX (Schering-Plough, Australia Pty Ltd, Sydney, NSW, Australia); Osmolite® (Abbott Nutrition, Australia Pty Ltd, Sydney, NSW, Australia; see the Electronic supplementary material) was used for the PF. The following concentrations were used for all experiments; TNF-α (100 ng/ml), HC (36 μg/ml) [13], IFX (1 in 137.5 dilution in media) [14] and PF (1 in 5 dilution in media). The concentrations of HC, IFX and PF [15] used in the current study were considered to represent a physiologic dilution. For some experiments, PF was also used at dilutions of 1:2.5 and 1:10.

Cell line, cell culture assay and TEER

The human epithelial colorectal adenocarcinoma cells Caco-2 (ATTC HTB-37) were used for all experiments. Caco-2 cells polarize in continuous culture and display differentiated cell structure and function in a monolayer format [16]. Culture media was minimum essential medium (MEM; Gibco Invitrogen, Carlsbad, CA, USA) containing 2 mM L-glutamine and supplemented with 20% heated-inactivated fetal bovine serum (FBS; Gibco), 1 M MEM non-essential amino acids (Gibco), 0.075 M sodium bicarbonate (Gibco), 1 mM sodium pyruvate (Gibco) and 100 U/ml penicillin/streptomycin (Gibco). Caco-2 cells were cultured at 37°C in 5% CO_2 in air within a humidified incubator until confluent. In each series of experiments, supernatants were harvested and stored at −80°C until assay. All experiments were repeated on at least five independent occasions.

For experiments requiring access to both apical and basolateral surfaces of the monolayer, Caco-2 cells were seeded at a density of 2×10^6 cells/ml in Transwell inserts

(0.4 μm pore size, with an exposed area of 144 mm^2; Corning Inc., Corning, NY, USA) or Bio-Coat inserts (collagen type 1 inserts, 24-well plates, 3.0 micron; BD Biosciences, Bedford, MA, USA) and cultured for 28–32 days, with media replaced every other day and transepithelial electrical resistance (TEER) measured regularly. TEER was measured using an EVOM epithelial volt-ohm meter (World Precision Instruments Inc., Sarasota, FL, USA). For measurements, both apical and basolateral compartments were bathed with Caco-2 media and the true monolayer resistance was determined according to the following equation:

Monolayer resistance = [Total monolayer resistance
   − Blank resistance (transwell without Caco-2 cells)]
   × Effective membrane area.

When TEER measurements plateaued above 250 Ω cm^2 [17], the cells were considered to be fully differentiated and were used for experiments. Experimental TEER measurements were taken prior to and after treatment. Each reported TEER value is the mean of five consecutive measurements.

Estimation of cell viability by trypan blue

Cells were washed twice with warm Dulbecco's phosphate buffer saline (PBS; Gibco) 1× and then incubated with 0.25% trypsin–EDTA (Gibco) for 15 min, with cell viability assessed by trypan blue exclusion, as described previously [15]. Live (clear) and dead (blue) cells were counted under the 40× objective of the light microscope (Nikon, Japan), with cell number and viability calculated using a haemocytometer (Brand, Germany). The means of three independent cell counts were pooled for analysis.

Measurement of interleukin (IL)-8 by enzyme-linked immunosorbent assay (ELISA)

IL-8 levels in supernatants were measured using the human IL-8 CytoSet kit (Invitrogen), according to the manufacturer's instructions. This antibody pair kit comes with matched antibody pairs to detect and quantify protein levels of human IL-8 using a sandwich ELISA. The lower detection limit of the assay is 15.6 pg/ml.

Assessment of short circuit current (Isc)
using an Ussing chamber

Caco-2 cells grown on Transwell inserts were placed in an Ussing chamber and kept under the following conditions for 1 h and 30 min: Caco-2 monolayers were bathed in

37°C oxygenated buffer [10 ml on both apical and basolateral sides] comprising 116 mM NaCl, 5.4 nM KCl, 0.4 mM MgCl$_2$, 1.8 mM CaCl$_2$, 5.5 mM glucose, 26 mM NaHCO$_3$ and 0.9 mM NaH$_2$PO$_4$ at a pH of 7.35. Voltage and current electrodes (EKV and EKC respectively; World Precision Instruments Inc.) were connected to a KCl-saturated agar bridge to monitor Isc. Following equilibration for 30 min, the Isc (μA/Cm^2) was continually measured with the voltage clamped at a potential difference of zero. The Isc integrity of the monolayers was calculated according to Ohm's law ($V = IR$) [18].

Horseradish peroxidise (HRP) flux measurements

In addition to electrophysiological measurements, monolayer permeability was assessed by HRP (a 44 kDa protein) flux. Following equilibration of the membrane in the Ussing chamber, 10^{-5} M of HRP were added to the apical buffer. Five hundred microlitre samples from apical and basolateral buffers were then taken at 15 min intervals over the course of 1 h and replaced with fresh buffer to maintain constant volume. Intact HRP was quantitatively assessed using a modified kinetic assay. Briefly, 150 μl of sample were mixed with 0.8 ml reaction mixture containing 0.003% H$_2$O$_2$ (MERK, Victoria, Australia) and 0.009% o-dianisidine dihydrochloric acid (Sigma). HRP catalytic rates were measured by spectrophotometery (Bio-Rad) using monochromatic light at a wavelength of 460 nm. HRP concentrations were calculated by comparing to a range of known standard HRP concentrations.

Fluorescent labelling of tight junction proteins

Caco-2 cells grown to confluence on collagen-coated glass slides (BD Biosciences, Franklin Lakes, NJ, USA) were incubated with or without TNF-α, and HC, IFX or PF (at a dilution of 1:5 in media) for 9 h. Afterwards, the cells were fixed with ice-cold methanol (Fronine Laboratory Supplies, Riverstone, Australia) for 15 min at room temperature and then rinsed three times with PBS before being blocked with 10% normal goat serum (Sigma) in 0.1% bovine serum albumin (BSA; Sigma) in PBS for 20 min at room temperature. Cells were washed with PBS and incubated overnight at 4°C with rabbit anti-occludin (1:1000 dilution; Zymed Laboratories, South San Francisco, CA, USA), rabbit anti-claudin-1 (1:1000 dilution; Zymed), rabbit anti-ZO-1 (1:500 dilution; Zymed) or normal rabbit serum (1:1000 dilution, Sigma) for staining controls. Cells were washed thoroughly with PBS and incubated with ALEXA 594 goat anti-rabbit IgG (1:200 v/v in BSA/PBS; Molecular Probes, Eugene, OR, USA) in the dark for 2 h at room

temperature. Slides were then washed with PBS and mounted with Vectashield mounting medium (Vector Laboratories, Burlingame, CA, USA). Fluorescent images were captured using an Axioplan 2 microscope (Zeiss, Oberkochen, Germany) and AxioVision software (Zeiss).

RNA purification and cDNA preparation assay

Following experimentation, confluent Caco-2 monolayers on inserts were washed with PBS, and then the total RNA was extracted by the Trizol reagent (Invitrogen), following the manufacturer's protocol. Contaminating DNA was removed using the Turbo DNA-free kit (Ambion, Austin, TX, USA) according to the manufacturer's protocol. Total RNA concentration and quality was evaluated by absorbance at 260/280 nm using a NanoDrop-1000 spectrophotometer (NanoDrop Technologies, Wilmington, DE, USA). Extracted RNA was reverse transcribed into cDNA using Superscript III reverse transcriptase (Invitrogen), following the manufacturer's protocol. Reactions were performed in a thermocycler (Corbett Research, Mortlake, Australia).

Quantification of gene expression by real-time (RT) polymerase chain reaction (PCR)

Each RT-PCR reaction contained nuclease-free water (Ambion), 12.5 μl of $1\times$ iQ^{TM} SYBER Green PCR buffer (Bio-Rad), forward and reverse primers (Table 1) and 5 μl of cDNA (2 ng/μl) as a template (or water as a negative control) in a total volume of 25 μl. RT-PCR for occludin, claudin-1 and ZO-1 was performed with an initial hot start step of 2 min at 95°C, followed by 40 cycles of 95°C for 20 s, 63°C for 30 s and 72°C for 60 s, or 40 cycles of 95°C for 15 s and 60°C for 1 min for MLCK. Reactions were performed on a Realplex Mastercycler (Eppendorf, Barkhausenwig, Hamburg, Germany) and analysed with Realplex software. Following PCR, amplification products were examined for homogeneity by melting curve analysis, with mRNA expression calculated using the $2^{-\Delta\Delta \text{ cycle threshold (Ct)}}$ method normalized against β_2-microglobulin (β_2M). Each

sample was run in triplicate with final values calculated as an average.

Sodium dodecyl sulfate polyacrylamide gel electrophoresis (SDS-PAGE) and western blotting

Western blotting was used to ascertain cytosolic (soluble) and membrane (insoluble) localisation of tight junction proteins using the method described by Wroblewski et al. [19.]. In brief, 2×10^6 Caco-2 cells were seeded in six-well plates (Becton Dickinson Labware, Franklin Lakes, NJ, USA) and cultured for 7 days until confluent, then co-cultured with or without TNF-α (in the basal side) and either HC, IFX or PF (1:5 dilution; in the apical side) for a further 9 h. Cells were lysed in Triton X-100 lysis buffer (150 mM NaCl, 50 mM Tris-Cl, pH 7.6, 0.5% Triton x-100 with protease inhibitors aprotinin and leupeptin) and centrifuged at $1400\times g$ for 10 min. Supernatants were collected as the cytosolic fraction, with pellets resuspended in lysis buffer containing 0.02% SDS for 30 min at 4°C. Samples were again centrifuged for 10 min at $1400\times g$, with supernatants collected as the membrane fraction.

Protein concentrations in supernatants were measured using the bicinchoninic acid method (Pierce, Rockford, IL, USA), fractionated on SDS-PAGE, then transferred to a polyvinylidene difluoride (PVDE) membrane using the mini-PROTEAN® Trans-Blot system (BioRad). Membranes were incubated with rabbit anti-occludin (1:400; Zymed Laboratories) or rabbit anti-claudin-1 (1:1000; Zymed Laboratories) or rabbit anti-ZO-1 (1:200; Zymed Laboratories) as primary antibodies, and goat anti-rabbit-IgG (Sigma) coupled to HRP as a secondary antibody. Proteins were detected using the 5-bromo-4-chloro-3-indolyl phosphate (BCIP)/nitro blue tetrazoluim (NBT) detection kit (Promega Corp., Madison, WI, USA), according to the manufacturer's instructions.

Statistical analysis

GraphPad Prism version 4.0 for Windows (GraphPad Software, San Diego, CA, USA) was utilized to generate graphs and to perform statistical analysis. All experimental

Table 1 Primer sequences utilized for real-time PCR

Gene	Forward primer	Reverse primer
Claudin-1 [35]	GCGCGATATTTCTTCTTGCAGG	TTCGTACCTGGCATTGACTGG
Occludin [36]	CGGTCTAGGACGCAGCAGAT	AAGAGGCCTGGATGACATGG
Zonula occludens (ZO-1) [36]	CGAGTTGCAATGGTTAACGGA	TCAGGATCAGGACGACTTACTGG
β_2-Microglobulin (β_2M)	AGGCTATCCAGCGTACTCCAAAGA	CGGATGGATGAAACCCAGACACAT
Long myosin light chain kinase (MLCK) [37]	AACGAGATCAACATCATGAACCA	CAGCTGTGCTTGCTCTCGAA

data values were expressed as the mean ± SD and ana-lysed using Student's unpaired t test, paired t test or ANOVA, as appropriate. p values of <0.05 were consid-ered significant.

Results

Assessment of cell viability and IL-8 secretion in response to TNF-α stimulation

The effect of TNF-α on cell viability was assessed. Caco-2 cells were exposed to TNF-α (100 ng/ml) for up to 48 h. Forty-eight hours of exposure to TNF-α resulted in decreased viability of the cells compared to the cells incubated without TNF-α (media-no-TNF-α controls; $p = 0.009$). However, no significant change in cell survival was noted for 9 h of incubation ($p = 0.1$). Next, the IL-8 secretion profile (an indicator of inflammation) was investigated. Caco-2 cells were incubated with 100 ng/ml of TNF-α for up to 48 h with supernatants collected for IL-8 measurement. TNF-α increased IL-8 secretion in a time-dependent manner compared to the media-no-TNF-α controls ($p = 0.003$). The maximal IL-8 response was reached after 9 h of incubation of the cells with TNF-α (data not shown). Nine hours of TNF-α incubation were used for all subsequent experiments.

Viability and IL-8 response in cells treated with HC, IFX or PF

In the following studies, we examined the possibility that the effect of HC, IFX or PF on Caco-2 cell monolayers on inserts in the presence or absence of TNF-α. Initially, cell monolayers were exposed to HC, IFX or PF (at 1:2.5, 1:5 and 1:10 dilutions) without TNF-α for 9 h. There was no decrease in cell viability for any of the treatments (data not shown). Supernatant IL-8 levels were also measured, and there was no increase in IL-8 levels compared to the media-no-TNF-α controls for any of the treatments following the incubation period (data not shown).

Next, cell monolayers were incubated with HC, IFX or PF (at 1:2.5, 1:5 and 1:10 dilutions) on the apical mono-layer side and TNF-α on the basal monolayer side. There was no decrease in cell viability with any of the treatments following incubation (data not shown). Supernatant IL-8 in cells exposed to TNF-α and media only were significantly elevated (media-TNF-α controls; 814 ± 9 pg/ml) com-pared to the media-no-TNF-α controls (403 ± 5 pg/ml; $p < 0.001$). Notably, cells incubated with IFX or PF (at a dilution of 1:5 or 1:10) had IL-8 levels equivalent to the media-no-TNF-α controls (IFX: 400 ± 8, $p = 0.5$; PF (1:5): 394 ± 8, $p = 0.1$; PF (1:10): 398 ± 8, $p = 0.2$).

Further, cells incubated with HC or PF (at 1:2.5 dilution) had reduced IL-8 levels compared to the media-TNF-α controls ($p = 0.041$ and $p = 0.023$, respectively), but were elevated compared to IFX ($p = 0.032$ and $p = 0.031$ respectively), PF (1:5 dilution; $p = 0.011$, $p = 0.044$ and 1:10 dilution; $p = 0.014$, $p = 0.012$, respectively) and media-no-TNF-α controls ($p = 0.021$ and $p = 0.034$, respectively).

Epithelial barrier function in cells treated with HC, IFX or PF

Cell monolayers grown on membrane supports were exposed to treatments (HC, IFX or PF) apically and TNF-α basally and incubated for 9 h. TEER was measured before and after incubation. Initially, IFX or PF (1:2.5, 1:5 or 1:10 dilutions) incubated without TNF-α did not affect TEER (data not shown), but HC alone did reduce TEER ($p = 0.034$). The subsequent series of experiments inclu-ded TNF-α in the incubations. Following 9 h exposure to TNF-α, TEER values significantly decreased by 229 ± 11 Ω cm^2 ($p < 0.001$, Table 2) in the media-TNF-α controls. When HC was included apically and TNF-α basally, TEER dropped by 40 ± 22 Ω cm^2 ($p = 0.032$, Table 2). However, there was no change in TEER levels with IFX or PF (at 1:5 and 1:10 dilutions) apically and TNF-α basally (Table 2). Interestingly, with PF at 1:2.5 dilution and TNF-α, there was a slight albeit significant drop in TEER of 20 ± 3 Ω cm^2 ($p = 0.009$, Table 2).

Following the TEER analysis, monolayers were then placed into an Ussing chamber and Isc and HRP flux were monitored for 1 h. Monolayers incubated with IFX or PF (all dilutions) without TNF-α had Isc ($p = 0.7$ and $p = 0.5$) and HRP flux levels ($p = 0.2$ and $p = 0.7$) equivalent to the media-no-TNF-α control monolayers. Similar to the TEER results, monolayers incubated with HC alone had slight but significantly elevated Isc compared to the media-no-TNF-α controls ($p = 0.043$). Next, the monolayers incubated with TNF-α were assessed. The media-TNF-α control monolayers had significantly higher Isc (389 ± 25 µA/Cm^2 h) compared to the media-no-TNF-α monolayers (155 ± 19 µA/Cm^2; $p < 0.001$; Fig. 1). Similar to the TEER results, monolayers incubated with IFX or PF (1:5 dilution) on the apical side and TNF-α on the basal side had Isc equivalent to the media-no-TNF-α control levels (Fig. 1). Further, monolayers incubated with HC and TNF-α had Isc levels below the media-TNF-α controls, but elevated compared to the media-no-TNF-α controls (Fig. 1).

For HRP flux, IFX, nor PF (all dilutions) and interest-ingly HC alone did not affect HRP flux when compared to the media-no-TNF-α controls ($p = 0.3$, $p = 0.6$ and $p = 0.2$, respectively). HRP flux in media-TNF-α controls

Table 2 Transepithelial electrical resistance (TEER) of stimulated/treated Caco-2 cells

Treatment	ΔTEER (Ω cm^2)[a]	p value
Media-TNF-α controls vs. media-no-TNF-α controls	**-229 ± 11**	**<0.001**
TNF-α + HC vs. media-no-TNF-α controls	**-40 ± 22**	**0.032**
TNF-α + IFX vs. media-no-TNF-α controls	$+12 \pm 11$	0.2
TNF-α + PF (1:2.5 dilution) vs. media-no-TNF-α controls	**-20 ± 3**	**0.009**
TNF-α + PF (1:5 dilution) vs. media-no-TNF-α controls	-3 ± 1	0.6
TNF-α + PF (1:10 dilution) vs. media-no-TNF-α controls	$+6 \pm 1$	0.1

Data are mean values $\pm$ SD from five independent experiments; Bold indicates statistical significance

[a] ΔTEER: post-treatment TEER $-$ pre-treatment TEER
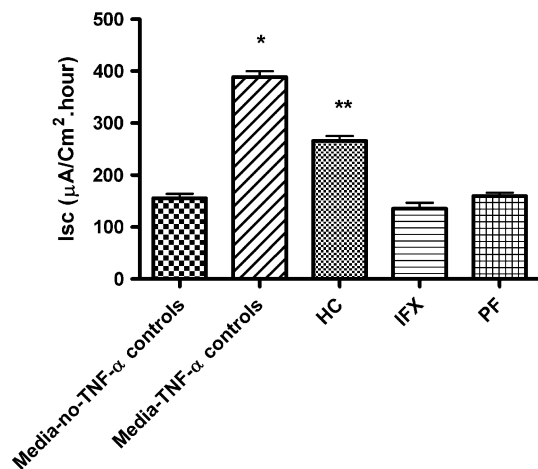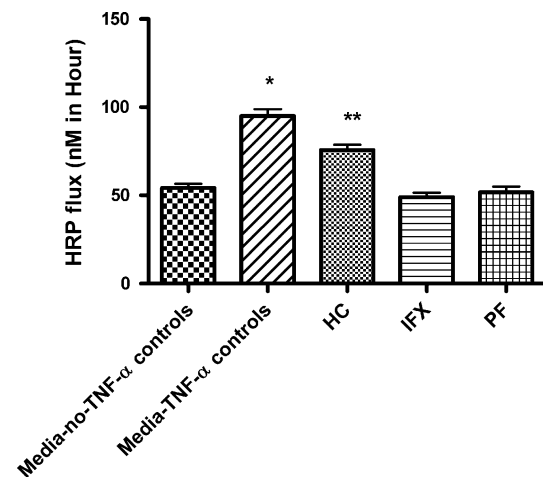

Fig. 1 Short-circuit current (Isc) in Caco-2 monolayers. Caco-2 monolayers on membrane supports were incubated with media alone (media-no-TNF-α controls), TNF-α alone (media-TNF-α controls), TNF-α + HC (HC), TNF-α + IFX (IFX) or TNF-α + PF at a dilution of 1 in 5 in media (PF) for 9 h, placed in an Ussing chamber, and the Isc was measured. Isc was elevated in the TNF-α incubated cells compared to the media-no-TNF-α controls (*$p < 0.001$). In addition, Isc was elevated in the TNF-α + HC cells compared to the media-no-TNF-α controls (**$p < 0.001$), but incubation with TNF-α + IFX or TNF-α + PF did not affect Isc compared to the media-no-TNF-α controls ($p = 0.2$ and $p = 0.7$, respectively). *TNF-α* tumor necrosis factor-α, *HC* hydrocortisone, *IFX* infliximab, *PF* polymeric formula

(95 $\pm$ 9 nM/h) was elevated compared to the media-no-TNF-α controls (54 $\pm$ 5 nM/h; $p < 0.001$; Fig. 2). Similar to the TEER and Isc results, monolayers incubated with IFX or PF (1:5 dilution) on the apical compartment and TNF-α on the basal compartment had HRP flux levels equivalent to the media-no-TNF-α controls (Fig. 2). With HC and TNF-α, monolayers had lower HRP flux levels compared to the media-TNF-α controls, but elevated levels compared to the media-no-TNF-α controls (Fig. 2).

Morphological distribution of tight junction proteins

In the media-no-TNF-α controls, tight junction staining appeared as continuous peri-cellular bands with clear cell

Fig. 2 Horseradish peroxidase (HRP) flux in Caco-2 monolayers. Caco-2 monolayers on membrane supports were incubated with media alone (media-no-TNF-α controls), TNF-α alone (media-TNF-α controls), TNF-α + HC (HC), TNF-α + IFX (IFX) or TNF-α + PF at a dilution of 1 in 5 in media (PF) for 9 h, and then placed in an Ussing chamber. HRP (10^{-5} M) was added to the apical side reservoir. Periodic samples were collected from both apical and basolateral reservoirs over a period of 1 h, and the HRP concentrations were determined by enzymatic assay. HRP flux was elevated in cells incubated with TNF-α alone when compared to the media-no-TNF-α controls (*$p < 0.001$). HRP flux was also elevated in cells incubated with TNF-α + HC when compared to the media-no-TNF-α controls (**$p < 0.001$), but there was no difference in HRP flux in cells incubated with TNF-α + IFX or TNF-α + PF compared to the media-no-TNF-α controls ($p = 0.2$ and $p = 0.5$, respectively). *TNF-α* tumor necrosis factor-α, *HC* hydrocortisone, *IFX* infliximab, *PF* polymeric formula

borders (Fig. 3A). Following 9 h of TNF-α incubation, the tight junction staining became irregular, with clear breakages in the tight junction strands and displacement in the cell borders with intra-cellular pooling of occludin, claudin-1 and ZO-1 (Fig. 3B). With the inclusion of HC, there appeared to be a partial recovery of tight junction (Fig. 3C). However, following incubation with either IFX or PF (1:5 dilution), the morphological distribution of tight junction proteins appeared indistinguishable to that of the media-no-TNF-α controls, since occludin, claudin-1 and

Fig. 3 Morphological distribution of tight junction proteins in Caco-2 cells. Caco-2 cells were grown to confluence on slides and incubated with media alone (media-no-TNF-α controls; *A*), TNF-α alone (media-TNF-α controls; *B*), TNF-α + HC (*C*), TNF-α + IFX (*D*) or TNF-α + PF at a dilution of 1 in 5 in media (*E*) for 9 h. Following these incubations, the cells were fixed with methanol and then immunofluorescently stained for occludin, claudin-1 or ZO-1. TNF-α caused a morphological redistribution of tight junction proteins, with visible breaks appearing at the tight junction borders. Incubation with TNF-α + IFX or TNF-α + PF did not appear to alter tight junction structure. However, incubation with TNF-α + HC did appear to affect the tight junction border and the distribution of tight junction proteins. *TNF-α* tumor necrosis factor-α, *HC* hydrocortisone, *IFX* infliximab, *PF* polymeric formula
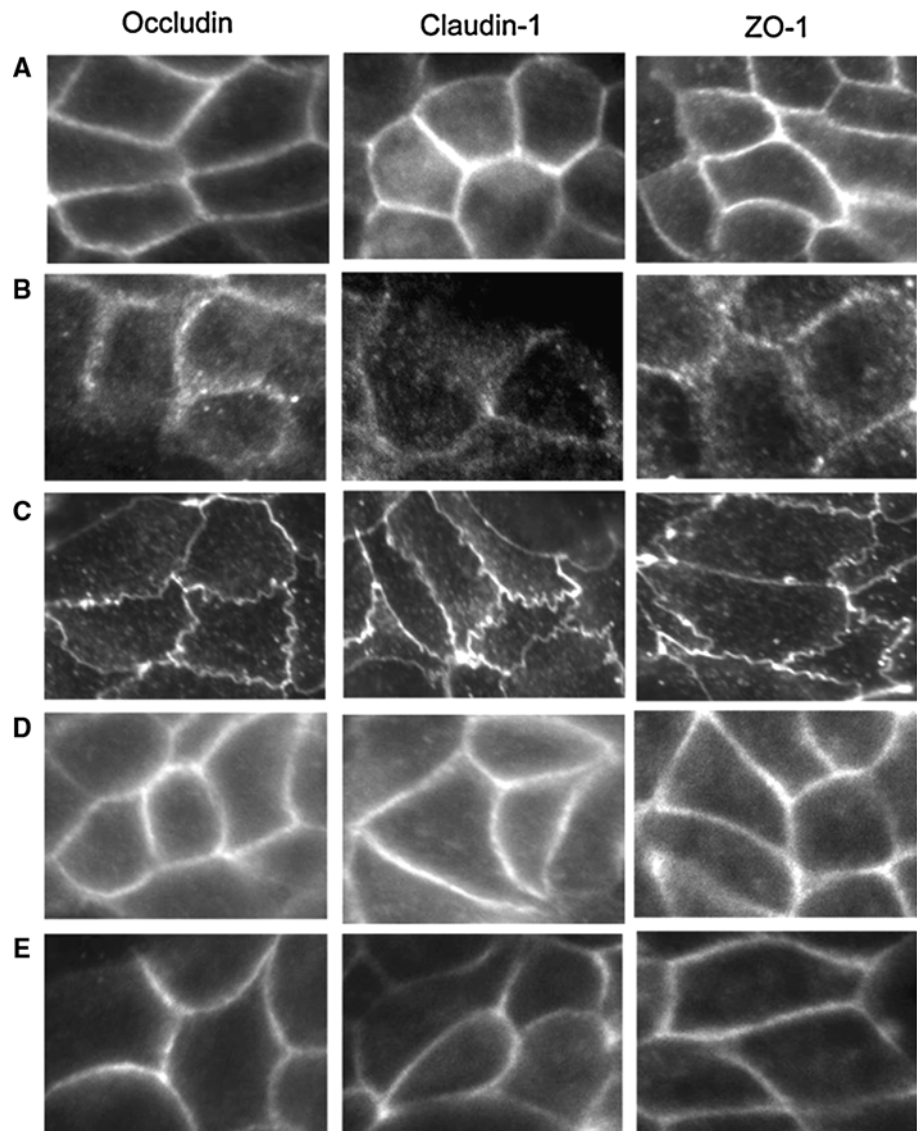
ZO-1 were sharply localized at the cellular margins (Fig. 3D, E).

Gene expression

mRNA expression of the tight junction associated genes occludin, claudin-1, ZO-1 and MLCK was assessed by real-time quantitative PCR. Gene expression was not affected by the presence of HC, IFX or PF (1:2.5, 1:5 or 1:10 dilutions) alone ($p > 0.05$). When monolayers were incubated with TNF-α, the mRNA expression of occludin, claudin-1 and ZO-1 significantly dropped but MLCK transcription increased dramatically compared to the media-no-TNF-α controls (Table 3). For monolayers incubated with PF (1:5 and 1:10 dilutions) and TNF-α, there was no change in the mRNA expression of any of the genes compared to the media-no-TNF-α controls (Table 3).

Interestingly, for PF at 1:2.5 dilution, gene expression of occludin, clauidn-1 and ZO-1 did fall slightly but significantly; however, MLCK mRNA expression increased by 0.71 ± 0.23 $\Delta\Delta$Ct ($p = 0.007$; Table 3). For monolayers incubated with IFX and TNF-α, gene expression was equivalent to the media-no-TNF-α controls, except for occludin, which was significantly lower (Table 3). In accordance with the epithelial barrier function and morphological distribution results, monolayers incubated with HC and TNF-α had significantly lower tight junction gene expression but higher MLCK mRNA expression (Table 3).

Membrane and cytoplasmic ZO-1 distribution

Western blotting was used to determine the membrane and cytoplasmic distribution of ZO-1. For the media-no-TNF-α control cells, ZO-1 was predominantly found in the

Table 3 Effect of TNF-α alone or in combination with HC, IFX or PF at different concentrations (1:2.5, 1:5 or 1:10) on the gene expression of occludin, claudin-1, ZO-1 and MLCK in the Caco-2 cell line

Treatment	p value			
	Occludin[a]	Claudin-1[a]	ZO-1[a]	MLCK[a]
Media-no-TNF-α controls	1.01 ± 0.11	1.05 ± 0.12	1.08 ± 0.16	1.01 ± 0.11
Media-TNF-α controls vs. media-no-TNF-α controls	**0.65 ± 0.09; p = 0.007**	**0.65 ± 0.07; p = 0.002**	**0.62 ± 0.10; p = 0.002**	**2.42 ± 0.48; p < 0.001**
TNF-α + HC vs. media-no-TNF-α controls	**0.83 ± 0.09; p = 0.009**	**0.85 ± 0.04; p = 0.017**	**0.84 ± 0.14; p = 0.032**	**2.31 ± 0.39; p < 0.001**
TNF-α + IFX vs. media-no-TNF-α controls	**0.82 ± 0.16; p = 0.033**	0.90 ± 0.12; p = 0.1	1.05 ± 0.04; p = 0.4	1.01 ± 0.09; p = 1.0
TNF-α + PF (1:2.5 dilution) vs. media-no-TNF-α controls	**0.88 ± 0.11; p = 0.033**	**0.79 ± 0.06; p = 0.008**	**0.81 ± 0.10; p = 0.013**	**1.72 ± 0.34; p = 0.007**
TNF-α + PF (1:5 dilution) vs. media-no-TNF-α controls	1.04 ± 0.08; p = 0.5	0.98 ± 0.07; p = 0.3	1.10 ± 0.10; p = 0.7	1.26 ± 0.25; p = 0.1
TNF-α + PF (1:10 dilution) vs. media-no-TNF-α controls	0.99 ± 0.06; p = 0.2	0.97 ± 0.03; p = 0.2	0.99 ± 0.05; p = 0.1	1.03 ± 0.07; p = 0.8

Data are mean values ± SD from four independent experiments; Bold indicates statistical significance

[a] ΔΔCt values

membrane, whereas for the media-TNF-α control cells, ZO-1 was predominantly in the cytosolic fraction (Fig. 4A, B). In cells incubated with HC and TNF-α, ZO-1 appeared to be equally distributed between the membrane and cytosolic fractions (Fig. 4C), whereas in cells incubated with IFX or PF (1:5 dilution) and TNF-α, ZO-1 was predominantly found in the membrane fraction (Fig. 4D, E).

Discussion

Although nutritional therapy is a well-established therapeutic method of inducing clinical remission in CD patients, there are limited studies elucidating the mechanisms of this safe therapy. Previous investigations into the clinical benefits of PF have been limited by a lack of reproducible intestinal epithelial cell models to elucidate the modulation of intestinal barrier function by PF. The current study has utilized Caco-2 monolayers to demonstrate—to the best of our knowledge for the first time—that PF is as effective as IFX and more effective than HC in rescuing intestinal tight junction integrity and preventing barrier dysfunction by maintaining normal TEER, Isc, permeability and the morphological distribution of tight junction proteins in the presence of the inflammatory cytokine TNF-α. This provides an elegant explanation as to why mucosal healing is achieved with IFX and nutritional therapy, but not with corticosteroid therapy.

The intestinal epithelium protects the body from antigens and noxious luminal substances by restricting the free passage of these molecules [1]. The mucosal layer and bilipid membrane of epithelial cells provide a barrier against water, ammonia and urea, while intracellular junctions (tight junctions and adherens junctions) form another barrier against the passage of larger molecules [20, 21]. The tight junction complex is composed of multiple components with adhesive functions, including transmembrane proteins (occludin and claudin) and cytoplasmic peripheral proteins such as ZO-1 [1, 3]. These junctions are crucial to the generation of electrical and chemical gradients that are important in the exchange of substances between internal and external cellular environments [21]. However, disturbances of tight junction barrier structure and function have been reported in some diseases, including CD. Several recent studies have investigated the effects of cytokines, and particularly TNF-α, upon tight junctions in the inflamed mucosa of patients with CD [2]. Based on available data, it is known that inflammatory changes are associated with elevated mucosal production of TNF-α and an increase in para-cellular permeability [1, 17, 18, 22]. Increased para-cellular permeability could occur for two reasons: epithelial cell apoptosis per se and/ or a loss of tight junction integrity.

A number of reports have proposed that increased epithelial cell apoptosis is the principal reason for enhanced epithelial permeability [23, 24]. However, other studies have shown that barrier function is maintained even when apoptosis is upregulated [3, 25], which may be a result of the rapid and dynamic repair of epithelial junctions by an actomyosin-dependent mechanism during the extrusion process [3, 26]. In regards to the second putative reason (loss of tight junction integrity), epithelial barrier dysfunction is considered to occur due to the redistribution of tight junction proteins [3, 17]. Dysregulation of tight
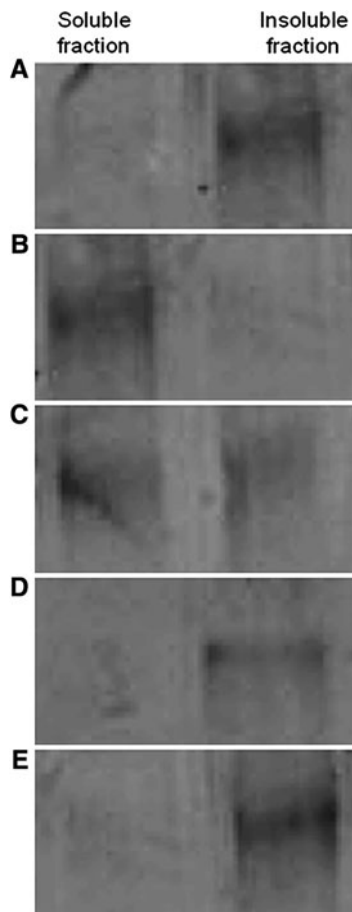
Fig. 4 Western blotting of zonula occludens (ZO)-1 in membrane and cytosol fractions. Caco-2 monolayers on membrane supports were incubated for 9 h with media alone (media-no-TNF-α controls; *A*), TNF-α alone (media-TNF-α controls; *B*), TNF-α + HC (*C*), TNF-α + IFX (*D*) or TNF-α + PF (*E*). Cells were then lysed, and the soluble (cytosol) and insoluble (membrane) fractions were collected and subjected to ZO-1 western blotting. The majority of the ZO-1 protein is membrane bound in the media-no-TNF-α controls, as ZO-1 is readily detectable in the membrane fraction but barely detectable in the cytosol fraction. TNF-α incubation redistributed ZO-1 to the cytosol; ZO-1 was then readily detectable in the cytosol fraction and barely detectable in the membrane fraction. TNF-α + HC does appear to cause redistribution of the ZO-1 protein, as ZO-1 appears to be equally detachable in both cytosol and membrane fractions. Incubation with TNF-α + IFX or TNF-α + PF does not appear to affect the ZO-1 distribution, as ZO-1 is predominantly detected in the membrane fractions, similar to the media-no-TNF-α controls. *TNF-α* tumor necrosis factor-α, *HC* hydrocortisone, *IFX* infliximab, *PF* polymeric formula, *ZO-1* zonula occludens-1

junction proteins and consequent barrier function may be predominantly associated with an increase in the phosphorylation of MLCK [3, 17]. MLCKs, both long and short isoforms, are the major effectors for the regulation of actomyosin function [17, 27]. It has been highlighted that TNF-α increases the transcription and translation of epithelial MLCK in an in vitro model [3, 17, 27]. When activated, MLCK reorganizes the distribution of tight junction proteins and induces barrier dysfunction [3, 17]. The involvement of MLCK in the disruption of tight junction barrier function and TJ permeability was further validated by siRNA targeted knock-down of MLCK expression [28, 29]. With near-complete depletion of MLCK protein in this model, the addition of IL-1β does not alter TEER and therefore does not affect epithelial barrier function [28, 29]. This suggests that inflammatory cytokine induced barrier dysfunction is associated with a mechanism involving MLCK. In addition, in vivo investigations have shown that MLCK protein expression is elevated in intestinal tissue from patients diagnosed with CD [28, 30]. Therefore, accumulating evidence indicates that MLCK expression is essential in intestinal epithelial barrier dysfunction.

In the present study, we have shown that gene expression of MLCK is elevated following the administration of TNF-α. Similarly, we have demonstrated that the enhanced transcription of MLCK is associated with a downregulation of the three main tight junction genes: occludin, claudin-1 and ZO-1. The Ussing chamber experiments clearly show that there is reduced barrier function following TNF-α incubation. Therefore, based on the available data, MLCK may be involved in barrier dysfunction by two possible mechanisms: reduction in tight junction gene expression or accelerated degradation and rearrangement of tight junction proteins.

The reduced tight junction strand complexity and an apparent increase in strand breaks were accompanied in the current study by upregulation of monolayer permeability, loss of TEER and increased epithelial Isc. All these changes reflected a loss of tight junction integrity and epithelial barrier dysfunction. Thus, it is clear that increased TNF-α leads to a leaky intestinal tight junction barrier, allowing the intestinal diffusion of luminal substances that may include bacteria and pathogens, and these can promote intestinal inflammation and mucosal injury [1, 31]. However, in CD it is not clear whether decreased barrier function precedes disease or is a result of active inflammation.

Various options are available for the medical treatment of patients with CD. Corticosteroids have been utilised as a primary treatment to induce remission in patients with CD for many years. Steroids are able to suppress the effects of proinflammatory cytokines, which may therefore improve intestinal tight junction permeability [7, 32]. However, corticosteroids are associated with a number of short- and long-term side effects [4, 11]. In the present study, HC partially reduced the effects of TNF-α-induced intestinal monolayer permeability. For instance, HC only partially prevented the downregulation of the gene expression of occludin, claudin-1 and ZO-1, as well as the upregulation of MLCK. Consistent with the gene expression results, we

also found that HC only partially abrogated the effects of TNF-α on tight junction protein expression and the morphological distributions of occludin, claudin-1 and ZO-1.

In addition to corticosteroid-based therapies, therapeutic strategies now include treatment with biologic anti-inflammatory therapies such as IFX. IFX neutralizes the effects of TNF-α and induces disease remission [33]. To date, it has been the most extensively studied biological agent used in the treatment of IBD. IFX was shown to downregulate the production of the pro-inflammatory cytokine TNF-α and to restore intestinal barrier function [20, 33]. In this study, we also found that IFX abrogated the effects of TNF-α such that epithelial barrier dysfunction was prevented. IFX modified the mRNA expression of MLCK, while the expression of occludin was partly modified. However, TEER remained completely normal following the administration of IFX with TNF-α incubation.

Over the last three decades, numerous studies have investigated the possible role of nutritional therapy in the management of patients with active CD [4, 9–11]. Children with active CD can be effectively treated by nutritional therapy for a period of 6–8 weeks [4, 10], leading to clinical remission rates equivalent to those gained with corticosteroids [9, 11]. Importantly, nutritional therapy also leads to very high rates of mucosal healing, two to three times greater than those seen with corticosteroids [9, 10]. Recently, Zhong et al. [34] demonstrated that intestinal barrier function is modulated following the administration of enteral nutrition supplemented with prebiotics and galactooligosaccharides in rats with severe acute pancreatitis. Consistent with these findings, the current study has shown that PF is more effective than HC at restoring tight junction integrity and epithelial barrier function in response to TNF-α stimulation in an in vitro model. Further, PF acted directly on epithelial cells to normalise TEER, Isc and monolayer permeability in TNF-α-stimulated cells. It also normalized the transcription of tight junction proteins whilst modifying the transcription of MLCK much more effectively than HC.

The mechanism(s) by which PF abrogates the effects of TNF-α is/are not known, although ongoing investigations in our laboratory are pursuing this objective. Previously, we have shown that PF delays the disassociation of IκB following an inflammatory stimulus [15]. Therefore, based on these previous findings, and noting that PF does not directly interact with TNF-α in our in vitro model, we speculate that PF may have direct anti-inflammatory properties exerted through the interruption of the NF-κB signalling pathway.

In conclusion, this study has re-established that TNF-α enhances barrier dysfunction, monolayer permeability and MLCK mRNA expression in cultured intestinal epithelial cells. These data also support a role for MLCK in the

disruption of tight junctions and the redistribution of the tight junction proteins occludin, claudin-1 and ZO-1. Moreover, the current study shows that IFX and PF act directly on epithelial cells to maintain normal tight junction structure and function in the presence of high levels of TNF-α, whereas HC only partially maintains tight junction structure and function. Therefore, these in vitro results support the hypothesis that PF is as effective as IFX, and more effective than HC, in resolving pro-inflammatory-induced barrier dysfunction. Further studies are required to define the intracellular mechanism(s) by which PF modulates the TNF-α response.

References

1. Forster C. Tight junctions and the modulation of barrier function in disease. Histochem Cell Biol. 2008;130:55–70.
2. Zeissig S, Burgel N, Gunzel D, Richter J, Mankertz J, Wahnschaffe U, et al. Changes in expression and distribution of claudin 2, 5 and 8 lead to discontinuous tight junctions and barrier dysfunction in active Crohn's disease. Gut. 2007;56:61–72.
3. Edelblum KL, Turner JR. The tight junction in inflammatory disease: communication breakdown. Curr Opin Pharmacol. 2009;9:715–20.
4. Day AS, Whitten KE, Sidler M, Lemberg DA. Systematic review: nutritional therapy in paediatric Crohn's disease. Aliment Pharmacol Ther. 2008;27:293–307.
5. de Ridder L, Rings EHHM, Damen GM, Kneepkens CMF, Schweizer JJ, Kokke FTM, et al. Infliximab dependency in pediatric Crohn's disease: long-term follow-up of an unselected cohort. Inflamm Bowel Dis. 2008;14:353–8.
6. Yee AM, Pochapin MB. Treatment of complicated sarcoidosis with infliximab anti-tumor necrosis factor-alpha therapy. Ann Intern Med. 2001;135:27–31.
7. Escher JC, Taminiau JAJM, Nieuwenhuis EES, Buller HA, Grand RJ. Treatment of inflammatory bowel disease in childhood: best available evidence. Inflamm Bowel Dis. 2003;9:34–58.
8. Rosh JR, Gross T, Mamula P, Griffiths A, Hyams J. Hepatosplenic T-cell lymphoma in adolescents and young adults with Crohn's disease: a cautionary tale? Inflamm Bowel Dis. 2007;13:1024–30.
9. Borrelli O, Cordischi L, Cirulli M, Paganelli M, Labalestra V, Uccini S, et al. Polymeric diet alone versus corticosteroids in the treatment of active pediatric Crohn's disease: a randomized controlled open-label trial. Clin Gastroenterol Hepatol. 2006;4:744–53.
10. Day AS, Whitten KE, de Jong NSH. Nutrition and nutritional management of Crohn's disease in children and adolescents. Curr Nutr Food Sci. 2006;2:3–14.
11. Berni Canani R, Terrin G, Borrelli O, Romano MT, Manguso F, Coruzzo A, et al. Short- and long-term therapeutic efficacy of

nutritional therapy and corticosteroids in paediatric Crohn's disease. Dig Liver Dis. 2006;38:381–7.

12. Fell JM, Paintin M, Arnaud-Battandier F, Beattie RM, Hollis A, Kitching P, et al. Mucosal healing and a fall in mucosal pro-inflammatory cytokine mRNA induced by a specific oral polymeric diet in paediatric Crohn's disease. Aliment Pharmacol Ther. 2000;14:281–9.

13. Forster C, Burek M, Romero IA, Weksler B, Couraud PO, Drenckhahn D. Differential effects of hydrocortisone and TNF-alpha on tight junction proteins in an in vitro model of the human blood–brain barrier. J Physiol. 2008;586:1937–49.

14. Baldassano R, Braegger CP, Escher JC, Dewoody K, Hendricks DF, Keenan GF, et al. Infliximab (REMICADE) therapy in the treatment of pediatric Crohn's disease. Am J Gastroenterol. 2003;98:833–8.

15. de Jong NSH, Leach ST, Day AS. Polymeric formula has direct anti-inflammatory effects on enterocytes in an in vitro model of intestinal inflammation. Dig Dis Sci. 2007;52:2029–36.

16. Gaillard JL, Finlay BB. Effect of cell polarization and differentiation on entry of *Listeria monocytogenes* into the enterocyte-like Caco-2 cell line. Infect Immun. 1996;64:1299–308.

17. Wang F, Graham WV, Wang Y, Witkowski ED, Schwarz BT, Turner JR. Interferon-gamma and tumor necrosis factor-alpha synergize to induce intestinal epithelial barrier dysfunction by up-regulating myosin light chain kinase expression. Am J Pathol. 2005;166:409–19.

18. Feighery LM, Cochrane SW, Quinn T, Baird AW, O'Toole D, Owens SE, et al. Myosin light chain kinase inhibition: correction of increased intestinal epithelial permeability in vitro. Pharm Res. 2008;25:1377–86.

19. Wroblewski LE, Shen L, Ogden S, Romero-Gallo J, Lapierre LA, Israel DA, et al. Helicobacter pylori dysregulation of gastric epithelial tight junctions by urease-mediated myosin II activation. Gastroenterology. 2009;136:236–46.

20. Fries W, Muja C, Crisafulli C, Cuzzocrea S, Mazzon E. Dynamics of enterocyte tight junctions: effect of experimental colitis and two different anti-TNF strategies. Am J Physiol Gastrointest Liver Physiol. 2008;294:G938–47.

21. Stevenson BR, Anderson JM, Bullivant S. The epithelial tight junction: structure, function and preliminary biochemical characterization. Mol Cell Biochem. 1988;83:129–45.

22. Gibson PR. Increased gut permeability in Crohn's disease: is TNF the link? Gut. 2004;53:1724–5.

23. Schulzke J-D, Bojarski C, Zeissig S, Heller F, Gitter AH, Fromm M. Disrupted barrier function through epithelial cell apoptosis. Ann N Y Acad Sci. 2006;1072:288–99.

24. Zeissig S, Bojarski C, Buergel N, Mankertz J, Zeitz M, Fromm M, et al. Downregulation of epithelial apoptosis and barrier repair in active Crohn's disease by tumour necrosis factor alpha antibody treatment. Gut. 2004;53:1295–302.

25. Watson AJ, Chu S, Sieck L, Gerasimenko O, Bullen T, Campbell F, et al. Epithelial barrier function in vivo is sustained despite gaps in epithelial layers. Gastroenterology. 2005;129:902–12.

26. Florian P, Schoneberg T, Schulzke JD, Fromm M, Gitter AH. Single-cell epithelial defects close rapidly by an actinomyosin purse string mechanism with functional tight junctions. J Physiol. 2002;545:485–99.

27. Graham WV, Wang F, Clayburgh DR, Cheng JX, Yoon B, Wang Y, et al. Tumor necrosis factor-induced long myosin light chain kinase transcription is regulated by differentiation-dependent signaling events. Characterization of the human long myosin light chain kinase promoter. J Biol Chem. 2006;281:26205–15.

28. Al-Sadi R, Ye D, Dokladny K, Ma TY. Mechanism of Il-1β-induced increase in intestinal epithelial tight junction permeability. J Immunol. 2008;180:5653–61.

29. Clayburgh DR, Rosen S, Witkowski ED, Wang F, Blair S, Dudek S, et al. A differentiation-dependent splice variant of myosin light chain kinase, MLCK1, regulates epithelial tight junction permeability. J Biol Chem. 2004;279:55506–13.

30. Weber CR, Turner JR. Inflammatory bowel disease: is it really just another break in the wall? Gut. 2007;56:6–8.

31. Ma TY, Tran D, Hoa N, Nguyen D, Merryfield M, Tarnawski A. Mechanism of extracellular calcium regulation of intestinal epithelial tight junction permeability: role of cytoskeletal involvement. Microsc Res Tech. 2000;51:156–68.

32. Vieira AT, Pinho V, Lepsch LB, Scavone C, Ribeiro IM, Tomassini T, et al. Mechanisms of the anti-inflammatory effects of the natural secosteroids physalins in a model of intestinal ischaemia and reperfusion injury. Br J Pharmacol. 2005;146:244–51.

33. Cury DHB, Costa JE, Irika K, Mijji L, Garcez A, Buchiguel C, et al. Protective effect of octreotide and infliximab in an experimental model of indomethacin-induced inflammatory bowel disease. Dig Dis Sci. 2008;53:2516–20.

34. Zhong Y, Cai D, Cai W, Geng S, Chen L, Han T. Protective effect of galactooligosaccharide-supplemented enteral nutrition on intestinal barrier function in rats with severe acute pancreatitis. Clin Nutr. 2009;28:575–80.

35. Halász J, Holczbauer A, Páska C, Kovács M, Benyó G, Verebély T, et al. Claudin-1 and claudin-2 differentiate fetal and embryonal components in human hepatoblastoma. Hum Pathol. 2006;37:555–61.

36. Orbán E, Szabó E, Lotz G, Kupcsulik P, Páska C, et al. Different expression of occludin and ZO-1 in primary and metastatic liver tumors. Pathol Oncol Res. 2008;14:299–306.

37. Ma TY, Boivin MA, Ye D, Pedram A, Said HM. Mechanism of TNF-{alpha} modulation of Caco-2 intestinal epithelial tight junction barrier: role of myosin light-chain kinase protein expression. Am J Physiol Gastrointest Liver Physiol. 2005;288:G422–30.